Carbohydrate Polymers 114 (2014) 170–178

Contents lists available at ScienceDirect

Carbohydrate Polymers

journal homepage: www.elsevier.com/locate/carbpol

Chitosan–starch nanocomposite particles as a drug carrier for the delivery of bis-desmethoxy curcumin analog

Sindhuja Bala Subramanian, Arul Prakash Francis, Thiyagarajan Devasena*

Centre for Nanoscience and Technology, A.C. Tech Campus, Anna University, Chennai 600025, Tamil Nadu, India

ARTICLE INFO

Article history:
Received 11 March 2014
Received in revised form 15 July 2014
Accepted 17 July 2014
Available online 1 August 2014

Keywords:
Drug delivery
Nanocomposite
Chitosan
Starch
BDMCA
MTT assay

ABSTRACT

The conventional drug delivery system has serious limitations such as lack of target specificity, altered effects and diminished potency. These limitations can be overcome by using biocompatible polymer as an effective drug delivery system. In this study, bis-demethoxy curcumin analog loaded Chitosan–starch (BDMCA–CS) nanocomposite particles were developed using different ratios of Chitosan and starch (3:1, 1:1 & 1:3) by ionic gelation method. The entrapment efficiency and drug loading capacity were found to be high for the formulation with the ratio 3:1 of BDMCA:CS. Physical characterization of the nanocomposite particles was determined using DLS and FTIR. The morphology of the BDMCA–CS nanocomposite particles were found to be spherical and regular by SEM analysis. In-vitro drug release profile of the BDMCA–CS nanocomposite particles showed a very slow and sustained diffusion controlled release of the drug. The cancer cells targeting ability of the BDMCA–CS nanocomposite particles were confirmed by performing MTT assay on MCF-7 breast cancer cell lines and VERO cell lines.

1. Introduction

Nanoparticles are usually referred as particles with a size ranging from 1 to 100 nm. They have completely new properties based on size, distribution and morphology (Jhan, 1999). Nanotechnology offers biological and clinical applications in terms of diagnosis, controlled drug delivery and imaging. It is possible to accumulate them for an extended period of time inside a cell which can improve diagnostic sensitivity and therapeutic efficiency (Vidyanathan, Kalishwaralal, Gopalram, & Gurunathan, 2009). These particles can penetrate across many biological barriers through small capillaries into individual cells, allowing a drug to accumulate at a target site in the body. But in addition to the biological applications, use of metal oxide nanoparticles in drug delivery could lead to oxidative stress, inflammation and damage to blood–brain barrier (BBB) (Francis, Dushendra Babu, Lavanya, Shenbaga Vidhya, & Devasena, 2011) in contrast to biocompatible and biodegradable non-toxic polymer. Therefore, there is a need for biocompatible nanoparticles with higher beneficiary effects and lower toxic nature.

Polymer nanoparticles offer the best results by encapsulating drugs and shows reduced toxicity by limiting the interaction of with healthy cells. Such delivery systems also have potential benefits such as controlled and long term release rates, enhanced bioactivity, reduced side effects, decreased administration frequency and ability to deliver multiple drugs to the same site. For example, chitosan nanoparticles have been reported as drug carrier for 5-Fluorouracil (Nagarwal, Singh, Kant, Maiti, & Pandit, 2011) and isoniazid (Muhammed Rafeeq, Junise, Saraswathi, Krishnan, & Dilip, 2010). Chitosan, the partially acetylated mucoadhesive and cationic (1–4)-2-amino-2-deoxy-β-D-glucan, is being used extensively as a drug carrier owing to its biocompatibility and biodegradability (Busilacchi, Gigante, Mattioli-Belmonte, & Muzzarelli, 2013; Muzzarelli, 2009, 2010; Muzzarelli et al., 2012; Thanou, Verhoef, & Junginger, 2001). It has antimicrobial and antitumor activities (Qin, Du, Xiao, Li, & Gao, 2002; Muzzarelli et al., 1990; Roller & Covill, 1999; Zheng & Zhu, 2003), owing to its unique characteristics, such as (i) higher affinity for negatively charged biological membranes and (ii) site-specific targeting in vivo, respectively (Calvo, Remunan-Lopez, Vila-Jato, & Alonso, 1997; Qi, Xu, Jiang, Hu, & Zou, 2004). By maintaining the optimum size, it accumulates in the tumor tissue via specific surface recognition (Debnath, Datta, Babu, Kumar, & Senthil, 2010). Previous studies have also reported that a combination of alginate, chitosan and pluronic F127 loaded with curcumin have improved properties such as solubility, encapsulation and dispersity of the drug (Das, Kasoju, & Bora, 2010) and chitosan–dextran sulphate complex have shown enhanced stability and increased mechanical strength (Chen, Vellore Mohanraj, Fang, & Heather Benson, 2007) than when used as individual polymer.

* Corresponding author. Tel.: +91 9962645151; fax: +91 44 22301656.
E-mail addresses: chindu14@gmail.com (S.B. Subramanian), fdapharma@gmail.com (A.P. Francis), tdevasenabio@gmail.com, tdevasenabio@annauniv.edu (T. Devasena).

http://dx.doi.org/10.1016/j.carbpol.2014.07.053
0144-8617/

Starch is a natural storage polymer of plants with unique properties such as biodegradability, low cost and renewability. It has been recently reported that starch based polymers have greater application in the biomedical field such as drug delivery systems and tissue engineering scaffolds (Baran, Mano, & Reis, 2004). The major drawback of starch is that it is poor in processability, dimensional stability and mechanical properties of its end products. Thus, starch has been reported to be used as a nanocomposite (Lu, Xiao, & Xu, 2009). It was interesting to note that the mechanical strength of chitosan-TPP beads increases on addition of starch granules (Venugopal, 2011). Bajer et al. have reported the intermolecular interactions between the chitosan and starch in their blend (Bajer & Kaczmarek, 2010). Thus we expect the formation of chitosan–starch composite carriers which may load the anticancer drug (BDMCA) and subsequently release the drug with high efficacy.

BDMCA stands for bis-desmethoxycurcumin analog, which is a curcuminoid of turmeric. In vitro and animal studies have reported that curcuminoids has antitumor (Aggarwal & Shishodia, 2006; Choi, Chun, Kim, Kim, & Park, 2006; Strofer, Jelkmann, & Depping, 2011), antioxidant, antiarthritic, antiamyloid, anti-ischemic (Shukla, Khanna, Ali, Khan, & Srimal, 2008) and anti-inflammatory properties (Stix, 2007). It has potential anticancer activity which stems from its ability to induce apoptosis in cancer cells without cytotoxic effects on healthy cells (Aggarwal & Shishodia, 2004). Studies have reported that Curcumin analogs show poor bioavailability due to poor absorption, rapid metabolism and rapid systemic elimination (Anand, Kunnumakkara, Newman, & Aggarwal, 2007). Therefore, there is a need for controlling release of this drug, through which good bioavailability can be achieved rapidly even at a lower dose.

Therefore, this investigation aims to synthesize a polymer nanocomposite using chitosan and starch loaded with BDMCA by ionic gelation technique and to determine (i) the drug (BDMCA) loading efficiency of the CS nanocomposite (ii) the drug entrapment efficiency of the CS nanocomposite (iii) the anticancer activity of BDMCA–CS nanocomposite against MCF-7 breast cancer cell line by MTT assay and (iv) cytotoxic activity of BDMCA–CS nanocomposite against VERO cell lines by MTT assay.

2. Materials and methods

2.1. Materials

Chitosan, starch and sodium tri poly phosphate were purchased from Sigma-Aldrich. Soluble starch was obtained from Hi Media and Tween-80 from Merck Specialties Pvt. Ltd., Mumbai and Glacial acetic acid from Thermo Fischer Scientific India Pvt. Ltd. Acetyl acetone, dimethyl formamide, diethanolamine and boric acid were purchased from Sisco Research Laboratories Pvt. Ltd. Salicylaldehyde was obtained from Merck Specialities Pvt. Ltd.

2.2. Methods

2.2.1. Preparation of BDMCA–CS nanocomposite particles

The chitosan–starch (CS) nanocomposite particles were synthesized using ionic gelation method (Calvo et al., 1997). Chitosan and soluble starch solutions were prepared in 2% Acetic acid. After the complete dissolution of chitosan and starch in acetic acid, few drops of 0.5% Tween-80 were added to the solution for uniform dispersion and to prevent aggregation at ambient temperature during stirring. BDMCA (bis-desmethoxy curcumin analog) was prepared using the protocol reported earlier (Babu & Rajasekaran, 2009). Briefly, to the mixture of acetyl acetone and boric acid, dimethyl formamide (DMF) was added in drops and heated for 15 min. This mixture was heated with salicylaldehyde for 5 min. A few drops of glacial acetic acid and diethanolamine mixture was added to this mixture and heated for 5 to 6 h. Kept it for overnight and then DMF was added and warmed to form a flow paste. This paste was added slowly into the 10% acetic acid and stirred for 2 to 3 h. After stirring, the mixture was sonicated for 15 min. Then the mixture was filtered in a Whatman No. 1 filter paper using a vacuum pump and dried on a watch glass at room temperature for 1–2 h. About 0.05% of chemically synthesized BDMCA was added to the CS nanocomposite. Finally, 1% sodium tri poly phosphate was added in drops to the solution as a cross linking agent until opalescence. The final suspension was centrifuged. The pelleted particles were then lyophilized at 5 mTorr and −54 °C for 8 h. These lyophilized particles were then denoted as BDMCA–CS nanocomposite particles. The BDMCA–CS nanocomposite particles were characterized by Particle size analysis, Scanning electron microscopy, Fourier transform infra-red spectroscopy. The BDMCA–CS nanocomposite particles were also analyzed for drug loading efficiency, in vitro drug release studies, cytotoxic activity and anticancer activity. The supernatant was used for the determination of drug entrapment efficiency. Different formulations of BDMCA–CS nanocomposite particles were prepared as shown in Table 1.

Table 1
Different formulations of BDMCA loaded chitosan–starch (CS) nanocomposite particles.

Formulation code	Chitosan (mg)	Starch (mg)	STPP (%)	Tween-80 (%)	BDMCA (mg)
BDMCA–CS 3:1	150	50	1	0.5	50
BDMCA–CS 1:1	100	100	1	0.5	50
BDMCA–CS 1:3	50	150	1	0.5	50

2.2.2. Physical characterization

The lyophilized BDMCA–CS nanocomposite particles were dispersed in distilled water and its particle size was measured using MALVERN ZETASIZER.

The scanning electron microscope (HITACHI model S3400N, Japan) was used to determine the surface morphology of nanocomposite particles. A drop of the well-dispersed sample was placed on a disc which was then air dried and scanned in a high vacuum chamber with a focused electron beam.

The infrared absorption bands of chitosan, starch, CS, BDMCA and BDMCA–CS nanocomposite particles were obtained using PERKIN ELMER Spectrum Rx1, USA. 1 mg each of chitosan, starch, CS, BDMCA and BDMCA–CS nanocomposite were ground in a mortar pestle along with KBr to make a small pellet of thickness 0.1 cm. KBr pellet was used as blank. Spectrum was observed in the scanning range of 400 to 4500 cm^{-1} with a resolution better than 0.7 cm^{-1} resolution. The peaks were used to identify the molecular components and structures.

2.2.3. Percentage drug content and drug encapsulation efficiency

About 2 mg of the lyophilized BDMCA–CS nanocomposite particles were dissolved in 10 ml Acetonitrile and centrifuged at 8000 rpm for 10 min. The acetonitrile solubilize the BDMCA alone to bring them out of the nanocapsules to be released into the supernatant. The absorbance of the supernatant was analyzed using UV–visible Spectrophotometer (T90+ UV/VISIBLE Spectrometer PG Instrument Ltd.) at 418 nm. The amount of BDMCA present in the supernatant was calculated using the calibration curve. From the calculated concentration of BDMCA, the percentage drug content was determined for all the three different formulations of BDMCA–CS using the following formula:

$$\text{percentage drug content} = \frac{\text{total amount of drug} \times 100}{\text{total weight of BDMCA} - \text{CS particles}}$$

After the incorporation of 0.05% BDMCA into the nanocomposite particles, the solution was centrifuged at 8000 rpm for 10 min. The photometric absorbance of the supernatant containing unloaded drug molecules was determined at the wavelength of 418 nm. The amount of BDMCA present in the supernatant was calculated by the formula: $Y = 0.0084X + 0.011$ using the calibration curve. From the calculated concentration of BDMCA, the encapsulation efficiency of the nanocomposite particles was determined for the three different formulations of BDMCA–CS nanocomposite particles using the following formula:

$$\text{encapsulation efficiency} = \frac{(\text{total amount of drug} - \text{amount of unbound drug}) \times 100}{\text{total amount of drug}}$$

The best two formulations of BDMCA–CS nanocomposite particles showing the high percentage drug content and high drug encapsulation efficiency were taken for in vitro drug release studies.

2.2.4. In vitro drug release studies

In vitro drug release studies of the BDMCA–CS nanocomposite particles were performed in a Franz-Diffusion cell containing phosphate buffer (pH 7.4) and using a dialysis membrane with a molecular weight cutoff (MWCO) of 10 kDa. The membrane was placed over the mouth of the cell, to which the nanocomposite particles were loaded. A magnetic peddle was placed in the cell and maintained at 100 rpm in a magnetic stirrer for uniform mixing. The entire setup was placed in a bowl filled with distilled water to maintain the temperature at 37.4 °C. About 2 ml of the solution was removed, using a syringe, from the Franz-Diffusion cell for every one hour and replaced with 2 ml of fresh phosphate buffer. The absorbance of the collected solution was measured using UV–visible spectrophotometer at 418 nm. From the absorbance value, the concentration of the BDMCA in the solution using a standard calibration curve. The formulation which shows slow and sustained drug release profile was taken for cytotoxic and anticancer assay studies.

2.2.5. Drug release kinetics

In order to understand the mechanism and kinetics of drug release, it is essential to fit the results of in vitro drug release study of well-known kinetic equations such as Zero order model (% cumulative drug release vs time), First order model (log % cumulative drug remaining vs time), Higuchi model (% cumulative drug release vs square root of time) and Hixson–Crowell model (cube root of % cumulative drug remaining vs time). Since our formulation is a polymeric system, the drug release data were further analyzed using Korsmeyer–Peppas model equation, $M_t/M_\infty = kt^n$, where M_t/M_∞ is the fraction of drug released at time t, k is release rate constant and n is the release exponent (Dash, Murthy, Nath, & Chowdhury, 2010).

2.2.6. Anticancer assay

The anticancer activity of the BDMCA–CS nanocomposite particles were checked on MCF-7 breast cancer cell lines and on VERO cell lines (kidney epithelial cells from African green monkey). Cells (1×10^5/well) were plated in 100 μl of medium (MEM) per well in 96 well titer plates (Hi media). After 48 h incubation at 37 °C the cell reaches the confluence. Then, the medium was removed and the monolayer of cells was washed twice with MEM. To the washed cell sheet 1 ml of the medium containing defined concentrations of BDMCA–CS nanocomposite particles were added in respective wells. Each dilutions of BDMCA–CS nanocomposite ranged from 1:1 to 1:64 and they were added to the respected wells of 96 well titer plates. The plates were incubated for 48 h at 37 °C in 5% CO_2. After incubation, the wells were decanted and washed with MEM for 2 to 3 times. Then, about 5 mg/ml concentration of MTT (3-(4,5-dimethyl-2-thiazolyl)-2,5-diphenyl-tetrazolium bromide) was added into the well (200 μl/well). After 4 h incubation, 100 μl of DMSO was added to each well and was incubated for 10 minutes. The presence of viable cells was then confirmed by the formation of purple color formazan crystals after adding solubilizing reagent (DMSO). The absorbance was measured at 594 nm colorimetrically. Cell viability was defined as the ratio (expressed as a percentage) of absorbance of treated cells to untreated cells.

$$\%\,\text{Cell viability} = \frac{\text{test absorbance}}{\text{control absorbance}} \times 100$$

The relative % Cell viability was obtained by plotting concentration along X-axis and cell viability along Y-axis.

Table 2
Size distribution of different formulations of BDMCA–CS nanocomposite particles.

Formulation code	Size of the particle (nm)
BDMCA–CS 3:1	320
BDMCA–CS 1:1	91
BDMCA–CS 1:3	170

3. Results

3.1. Particle size analysis (PSA)

The particle sizes of the BDMCA–CS nanocomposite particles of different formulations (3:1, 1:1 and 1:3) are shown in Table 2 and their dispersity is shown in Fig. 1a–c, respectively.

A maximum size of 320 nm was observed in the formulation BDMCA–CS 3:1 due to the higher concentration of chitosan. A size of 170 nm was observed in BDMCA–CS 1:3 due to increased concentration of starch. Uniform size distribution was obtained in all the three formulations. However, as the chitosan and starch concentration was reduced, the size of the nanocomposite particles got reduced with the least size of 91 nm in the formulation BDMCA–CS 1:1.

3.2. Scanning electron microscopy (SEM)

The SEM images of all the three formulations (BDMCA–CS 3:1, 1:1 & 1:3) are shown in Fig. 2a–c. The morphology of the BDMCA–CS nanocomposite particles were found to be spherical with smooth and regular surface for all the three formulations. The change in polymer concentration does not affect the morphology. Amongst all shapes spherical nanoparticles are best suited for drug delivery applications. (Venkatraman, Hedrick, Ong, & Yang, 2011). Reports suggest that the spherical nanoparticles have higher probability for cell entry (Zhang et al., 2012). Therefore, we report that the three formulations may be investigated for drug loading and drug encapsulation efficiency.

3.3. Fourier transform infrared spectroscopy (FTIR)

The IR spectrums of chitosan, starch, CS, BDMCA and BDMCA–CS nanocomposite particles were reported in the Fig. 3.

The IR spectrum of chitosan showed five characteristic peaks at 3451 cm^{-1} (—OH stretching), 2920 cm^{-1} (—CH stretching), 1647 cm^{-1} (—NH_2), 1382 cm^{-1} (—CO stretching of primary alcoholic group) and 1076 cm^{-1} (C—O—C stretching). These results coincide with the findings of Nagarwal et al. (2011).

The spectrum of starch showed peaks at 3402 cm^{-1} (—OH stretching), 2929 cm^{-1} (—CH stretching), 1159 cm^{-1} (—CO stretching), 997 cm^{-1} and 925 cm^{-1} (—COH bending), 1084 cm^{-1} and

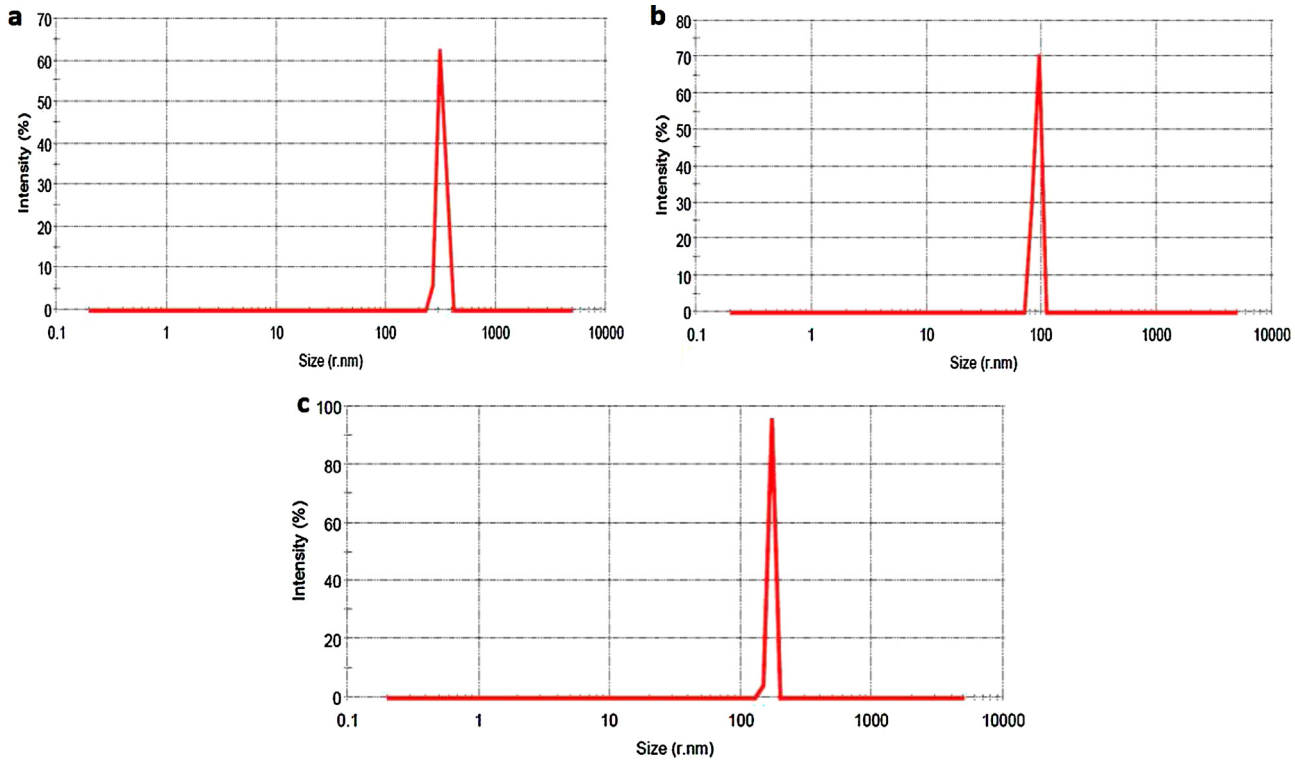

Fig. 1. Size dispersity of BDMCA–CS nanocomposite particles of ratio (a) 3:1, (b) 1:1 & (c) 1:3.

859 cm^{-1} (C—O—C symmetrical stretching). These results are found to be similar to the data reported earlier (Cael, Koenig, & Blackwell, 1973, 1975).

On comparison of IR spectrum of chitosan and starch with that of CS nanocomposite particles, we noticed that the absorption band owing to OH moiety has broadened at 3482 cm^{-1}. Kumari and Rani (2011) has implied that broadening of the OH stretch is an indication of intermolecular hydrogen bonding. We could, therefore, suggest that the chitosan is hydrogen bonded to starch. The 1647 cm^{-1} peak of $-NH_2$ group in chitosan shifts to 1654 cm^{-1}. This indicates that the phosphate group of tripolyphosphate is associated with ammonium groups of chitosan through electrostatic interactions to form the polyelectrolyte complex. Overall, the FTIR data of chitosan, starch and CS nanocomposite confirms that the

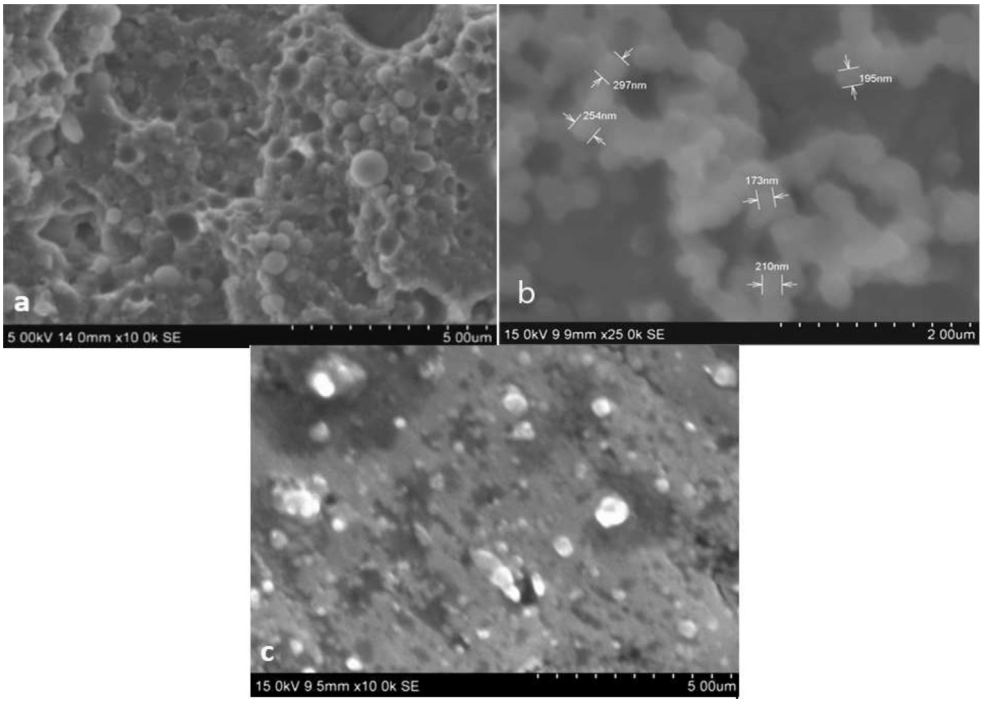

Fig. 2. SEM image of different ratios of nanocomposites (a) BDMCA–CS 3:1 (b) BDMCA–CS 1:1 (c) BDMCA–CS 1:3.

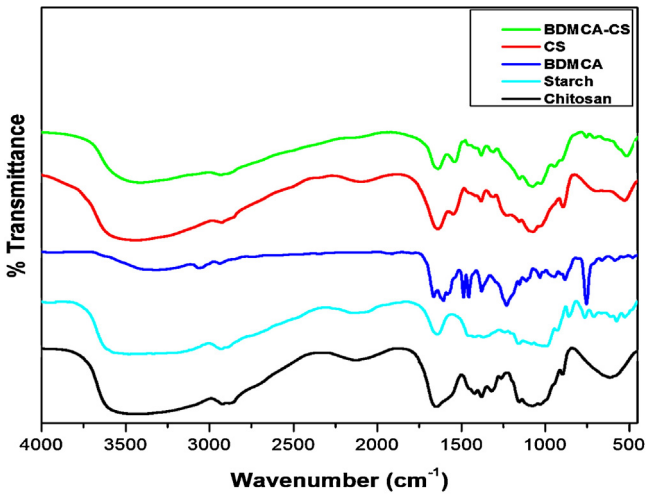

Fig. 3. FTIR Spectrum of chitosan, starch, CS nanocomposite, BDMCA and BDMCA–CS nanocomposite.

spherical particles (observed in SEM) are nanocomposite of chitosan and starch, gelated with TPP.

The FTIR spectrum of BDMCA shows O—H stretching at 3425 cm^{-1}, C=O stretching at 1614 cm^{-1} and 1230 cm^{-1}, C=C olefienic stretching and C=C aromatic stretching at 1505 cm^{-1} and 1449 cm^{-1}, respectively, and C=CH aromatic stretching at 756 cm^{-1}. These data corresponds to the functional groups present in BDMCA. These data are similar to those observed by Naama, Al-Temimi, and Ahmed (2010).

In the FTIR spectrum of BDMCA–CS nanocomposite, the peak corresponding to OH stretching has broadened (3456 cm^{-1}). This may be due to the interaction of BDMCA with the CS nanocomposite by means of hydrogen bonding. After the loading of BDMCA into the CS nanocomposite, a shift in the peak from 1654 cm^{-1} and 1382 cm^{-1} to 1626 cm^{-1} and 1378 cm^{-1}, respectively, was observed. It was also interesting to note that a similar range of peak shifts has already been reported by Das et al. (2010) suggesting the possibility of encapsulation of curcumin into the CS nanocomposite. Thus, it is logical to infer that the peak shift observed in our study signals that the drug BDMCA might have got encapsulated in the CS nanocomposite. Further, some extra peaks corresponding to the composite compound starch and the drug, BDMCA also appeared in the FTIR spectrum of BDMCA–CS. They are: (i) peaks at 1097 cm^{-1} and 887 cm^{-1} due to C—O—C symmetrical stretching of starch (ii) the peak at 756 cm^{-1} (C=—H aromatic stretching), 1451 cm^{-1} (C=C aromatic stretching) and 1239 cm^{-1} (C=O stretching) are the characteristic peaks of BDMCA. These peaks are Supportive data for confirming the presence of our drug BDMCA within the CS nanocomposite. For the most part, the FTIR spectrum of BDMCA–CS nanocomposite reveals that the drug got encapsulated within the CS nanocomposite.

3.4. Percentage drug content and drug encapsulation efficiency

The amount of drug per unit volume present in the formulation is the drug content. The amount of drug entrapped within the nanocarrier is its drug encapsulation efficiency. The percentage drug content and drug encapsulation efficiency are calculated with a constant amount of BDMCA (50 mg) but varying the ratio of chitosan and starch. The drug content was found to be 25.75%, 17.5% and 24.25% for the formulations BDMCA–CS 3:1, 1:1 and 1:3, respectively. The encapsulation efficiency was found to be 88.98%, 86.54% and 86.60% for the formulations BDMCA–CS 3:1, 1:1 and 1:3, respectively. Both the parameters showed maximum values

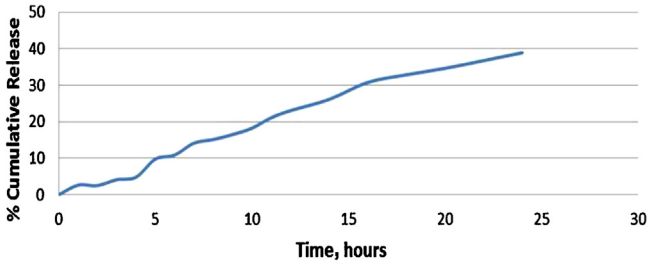

Fig. 4. In-vitro release profile of bis-demethoxy curcumin analog (BDMCA) from the formulation with chitosan: starch in the ratio of 3:1.

in the formulation BDMCA–CS 3:1. This may be attributed to the increased amount of chitosan since longer chain of chitosan can encapsulate larger amount of BDMCA in the presence of TPP as a cross linking agent. Only minor difference was observed in the encapsulation efficiency between BDMCA–CS 1:1 (86.54%) and 1:3 (86.60%), though the proportion of Starch was higher in the formulation BDMCA–CS 1:3. The second leading drug loading capacity was observed in BDMCA–CS 1:3 (24.25%). This may be due to the higher quantity of Starch. BDMCA–CS 1:1 (17.5%) had the least drug loading capacity as the shorter chains of Chitosan and Starch can load the minimum amount of BDMCA. We therefore interpret that the percentage drug content and drug encapsulation efficiency increases with increasing concentration of the polymer and the increase was more predominant with increasing concentration of chitosan.

3.5. In-vitro drug release studies

From our results discussed so far, it is obvious that the formulations BDMCA–CS 3:1 and 1:3 exhibit higher percentage drug content and drug encapsulation efficiency. We therefore used these two formulations for in-vitro drug release studies. The drug (BDMCA) release profile from the two formulations (BDMCA–CS 3:1 and 1:3) are shown in Figs. 4 and 5, respectively. The drug release profile showed a very slow release of BDMCA from the two different formulations for every one hour. Formulation BDMCA–CS 3:1 showed about 20% of the drug release in 10 h, 35% of drug release in 20 h and about 40% in 24 h. Whereas, the formulation BDMCA–CS 1:3 showed about 23% drug release in 10 h, 39% in 20 h and 45% release in 24 h. There was no initial burst release found in both the formulations. Though there was only minor difference between the release profiles of the two formulations, the formulation BDMCA–CS 3:1 showed a very slow release compared to BDMCA–CS 1:3. One of the primary criteria for passive targeting of cancer cells is that the drug delivery system should be capable of retaining the drug for a prolonged period of time, thus, facilitating a controlled and sustained release of the drug without any initial burst release (Das et al., 2010). Our results fulfill this criterion as we also observed a controlled release of BDMCA without any burst release. Thus, we expect that the chitosan–starch (CS)

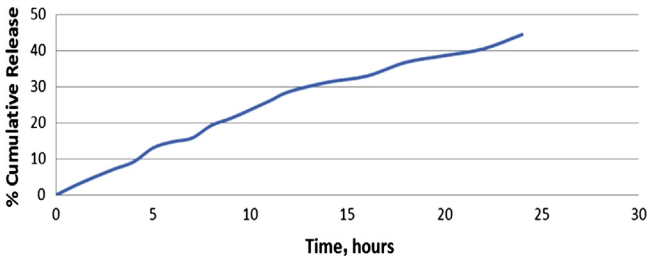

Fig. 5. In-vitro release profile of bis-demethoxy curcumin analog (BDMCA) from the formulation with chitosan: starch in the ratio of 1:3.

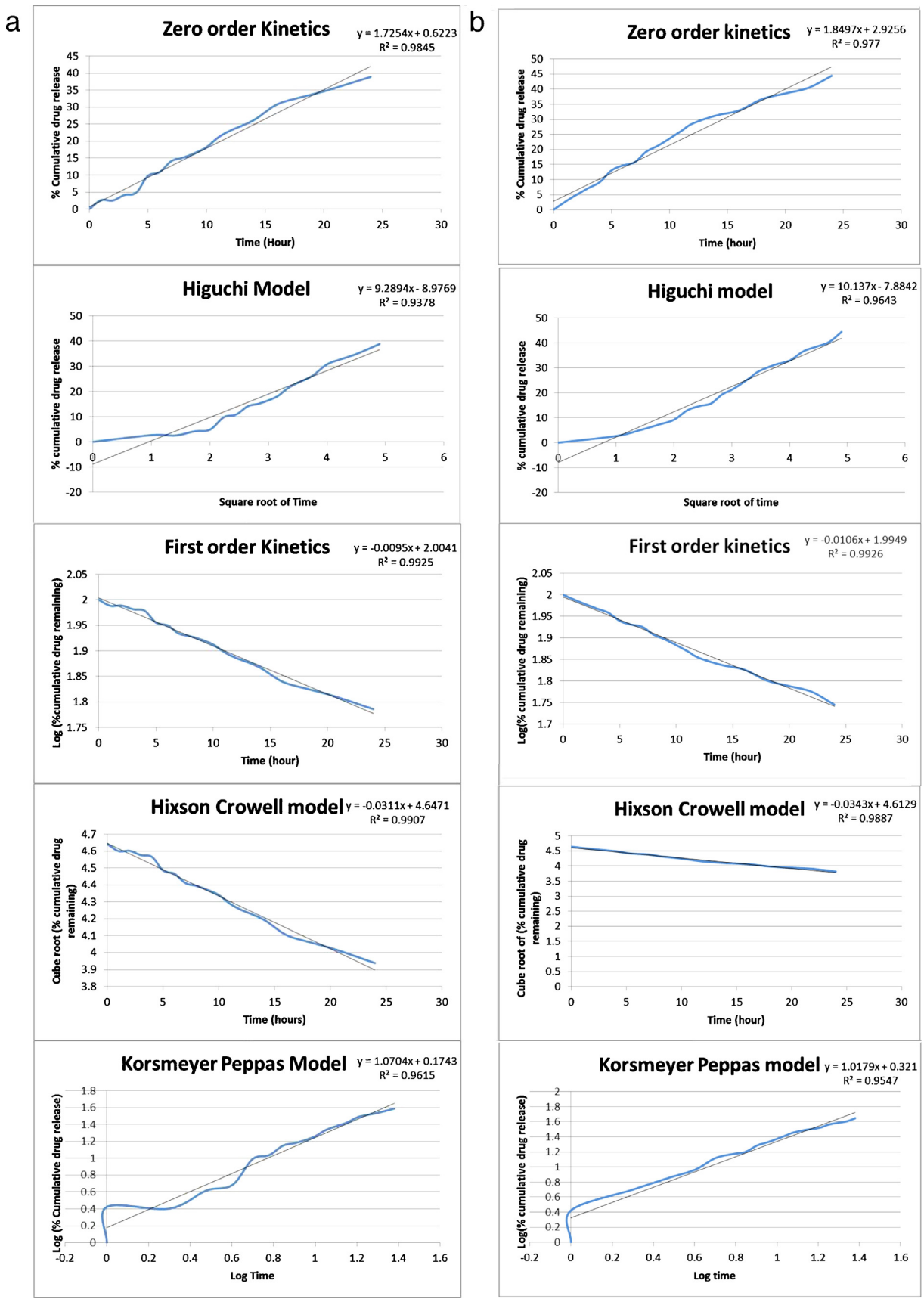

Fig. 6. Release kinetics of BDMCA from the formulation (a) BDMCA–CS 3:1 (b) BDMCA–CS 1:3.

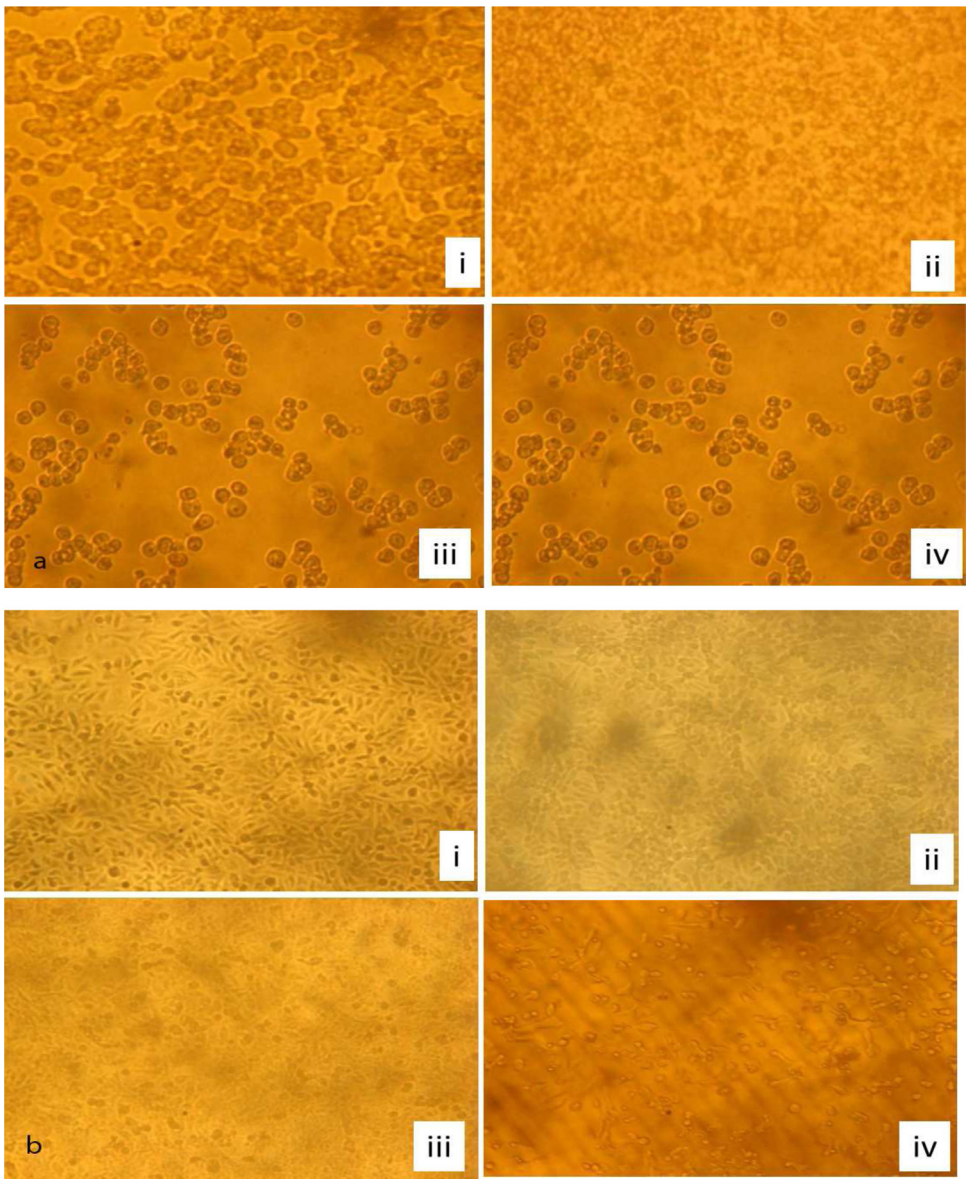

Fig. 7. (a) Morphology of MCF-7 cancer cells with BDMCA–CS nanocomposite particles. (i) Control; (ii) Cells treated with 62.5 μg/ml of BDMCA–CS; (iii) Cells treated with 250 μg/ml of BDMCA–CS; (iv) Cells treated with 1000 μg/ml of BDMCA–CS. (b) Morphology of VERO cells treated with BDMCA–CS nanocomposite particles. (i) Control; (ii) Cells treated with 62.5 μg/ml of BDMCA–CS; (iii) Cells treated with 250 μg/ml of BDMCA–CS; (iv) Cells treated with 1000 μg/ml of BDMCA–CS.

nanocomposite can be a perfect drug delivery tool for cancer cells. Therefore, we subsequently investigated the ability of CS nanocomposite particles to release BDMCA into breast cancer cells possibly via passive tumor targeting. Sustained drug release may be the reason for delayed saturation, as ob served by the absence of plateu in Figs. 4 and 5. The mechanism of drug release may be due to diffusion or polymer dissolution as explained in the next section.

3.6. Drug release kinetics

The release profile, i.e., the order and the mechanism of BDMCA release from the nanocomposite can be interpreted by different kinetic models such as, Zero order model, First order model, Higuchi's model, Korsmeyer–Peppas model and Hixson–Crowell model. Therefore, the kinetic release data of BDMCA–CS 3:1 (Fig. 6a) and 1:3 (Fig. 6b) were fitted into the Zero order model. First order model, Higuchi's model, Korsmeyer–Peppas model and Hixson–Crowell model.

The First order plot exhibited good linearity ($R^2 = 0.992$ for both the formulations, BDMCA–CS 3:1 and 1:3) when compared to Zero order plot ($R^2 = 0.984$ and 0.977 for BDMCA-CS 3:1 and 1:3, respectively). This shows that the amount of BDMCA released is dependent on the concentration of the drug loaded in the nanocomposite i.e., drug release is concentration dependent (Cho, Wang, Nie, Chen, & Shin, 2008).

We also observed good linearity in Higuchi plot ($R^2 = 0.937$ and 0.964 for BDMCA–CS 3:1 and 1:3, respectively). This observation clearly indicates that the drug release is due to diffusion mechanism.

The release of BDMCA from the CS nanocomposite exhibited a good fitting with Hixson–Crowell plot with a good linearity value ($R^2 = 0.990$ and 0.988 for BDMCA–CS 3:1 and 1:3, respectively). This shows that the BDMCA may be released due to polymer dissolution or erosion (Rahman et al., 2011).

The value of n in Korsmeyer–Peppas plot is 1.070 and 1.017 for BDMCA–CS 3:1 and 1:3, respectively. Dash et al. (2010) have suggested that an > 0.5 corresponds to Fickian diffusion mechanism,

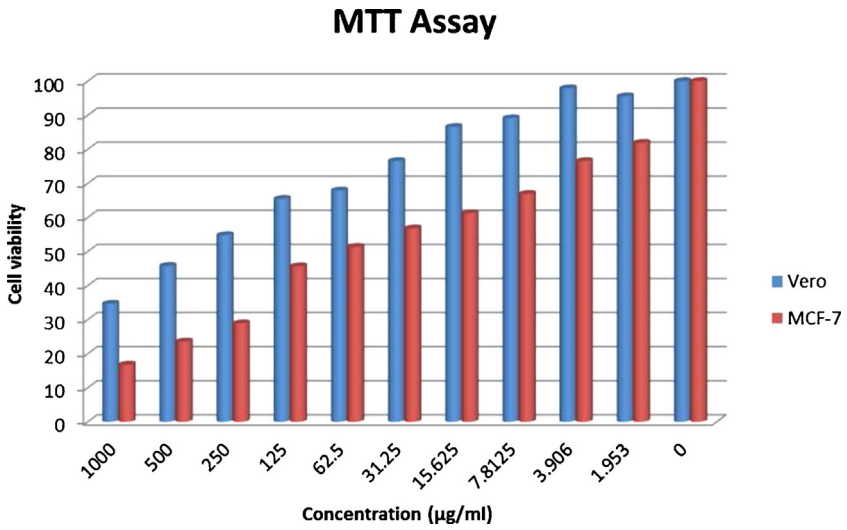

Fig. 8. Cell viability of MCF-7 and VERO cells at increasing concentration of BDMCA–CS nanocomposite.

$0.45 < n < 0.89$ corresponds to non-Fickian mechanism, $n = 0.89$ to relaxational transport (Case II) while $n > 0.89$ refers to Super case II transport. Thus, we suggest that the release of BDMCA form CS nanocomposite is Super case II transport.

3.7. Anticancer assay

Anticancer agents exert their activity by blocking the cell cycle progression and triggering apoptotic cell death. The half-maximal inhibitory concentration (IC_{50}) is the concentration of the anticancer agent that induces 50% of the cell death. The anticancer activity of BDMCA–CS nanocomposite particles was determined by performing MTT assay on MCF-7 and Vero cell lines after incubating these cells with different concentration of BDMCA–CS nanocomposite particles.

The MCF-7 and Vero cells were treated with different concentrations of BDMCA–CS nanocomposite particles (1.953, 3.906, 7.8125, 15.625, 31.25, 62.5, 125, 250, 500 and 1000 μg/ml). Microscopic images of BDMCA–CS treated and untreated (Control) MCF-7 and Vero cell lines are shown in Fig. 7a and b. The microscopic images revealed that the BDMCA–CS had a greater cytotoxic effect on MCF-7 cells than on Vero cells. MCF-7 cells treated with higher concentration of BDMCA–CS exhibited morphological changes such as membrane shrinkage, cell aggregation, detachment from the well surface and rounding up of cells. These morphological features indicate the BDMCA–CS induced cell death (Soundarajan & Sreenivasan, 2012).

A cell is said to be viable when the key enzyme, dehydrogenase present in the mitochondria of the cell, converts the yellow colored MTT dye into purple colored formazan crystals. Thus, the absorbance reading at 594 nm indicates the number of viable cells. The cell viability of MCF-7 and Vero cells against increasing concentration of BDMCA–CS nanocomposite particles are graphically represented in Fig. 8.

4. Discussion

We suggest that the size of the nanocomposite particles increases with increasing concentration of at least one of the polymers (320 to 91 nm). It has been reported that the size of the nanoparticles used in drug delivery applications should be large enough (100 to 600 nm) to prevent their leakage into blood capillaries but small enough (150 to 200 nm) to escape the reticuloendothelial system (Cho et al., 2008). This context is related to enhanced permeability and retention (EPR) effect. It is the property by which certain sizes of molecules typically liposomes, nanoparticles, and macromolecular drugs tend to accumulate in tumor tissue much more than they do in normal tissues. Therefore, we infer that all the three formulations prepared by us may further be analyzed for drug loading and drug encapsulation efficiency. Previous studies suggested that the spherical nanoparticles are best suited for drug delivery applications because they are capable of overcoming the limitations such as poor drug loading capacity, low drug efficacy, broad size distribution and non-specific drug toxicity (Cho et al., 2008). These findings coincide with our results, as the particles synthesized by us were also spherical. Thus, we suggest that the BDMCA loaded CS nanocomposites are good candidates for drug delivery. The FTIR data of chitosan, starch and CS nanocomposite confirms that the spherical particles (observed in SEM) are nanocomposite of chitosan and starch, gelated with TPP. Among the three ratios investigated, the percentage drug content and the drug encapsulation efficiency were found to be highest for the composite with highest proportion of chitosan.

First order, Korsmeyer–Peppas & Hixson–Crowell Kinetics plot of our study reveals a good linearity. Previous studies on sustained release of Ranolazine (Rahman et al., 2011) suggested that good linearity value in vitro model is an indicator of sustained drug release by both diffusion and polymeric erosion. These findings are in line with our reports revealing the dual mechanism involved in the release of BDMCA from CS nanocomposite. Thus we could suggest that CS nanocomposite may help with sustained release of BDMCA, which may be useful for many therapeutic applications. With these findings as a preliminary approach, we carried out cytotoxic assay (in Vero and MCF-7) to check the anticancer activity of CS-BDMCA. This may be a proof for the sustained release of BDMCA.

On comparing the cell viability of Vero and MCF-7 cells, it can be observed that the cell viability of the MCF-7 cells decreased at a higher rate as the concentration of the BDMCA–CS increased. Thus, it is obvious that BDMCA–CS functions as an anticancer agent by inducing cell death via cytotoxicity. Further, it was found that 62.5 μg/ml concentration of BDMCA–CS induced 50% of the MCF-7 cells (IC_{50}), whereas more than 250 μg/ml concentration of BDMCA–CS induced 50% cell death in Vero cells.

5. Conclusion

For the first time, we have formulated BDMCA loaded chitosan–starch nanocomposite for the controlled release of

BDMCA. The formulation BDMCA–CS 3:1 showed good drug entrapment efficiency and percentage drug content, followed by BDMCA–CS 1:3. These formulations showed sustained release of BDMCA. Subsequently, formulation BDMCA–CS 3:1 showed anticancer activity against the breast cancer cell lines (MCF-7). Release kinetics studies revealed that the release of BDMCA from the CS nanocomposite takes place by both diffusion and polymeric erosion. On the whole, we speculate that the CS nanocomposite of ratio 3:1 can be a better delivery tool for BDMCA to treat breast cancer. The effect of this formulation of other cancer models is underway in our laboratory.

References

Aggarwal, B. B., & Shishodia, S. (2004). Suppression of the nuclear factor-κB activation pathway by spice-derived phytochemicals: Reasoning for seasoning. *Annals of the New York Academy of Sciences*, *1030*, 434–441.

Aggarwal, B. B., & Shishodia, S. (2006). Molecular targets of dietary agents for prevention and therapy of cancer. *Biochemical Pharmacology*, *71*, 1397–1421.

Anand, P., Kunnumakkara, A. B., Newman, R. A., & Aggarwal, B. B. (2007). Bioavailability of curcumin: Problems and promises. *Molecular Pharmaceutics*, *4*, 807–818.

Babu, K. V. D., & Rajasekaran, K. N. (2009). Simplified conditions for the synthesis of curcumin and other curcuminoids. *Organic Preparations and Procedures International*, *26*, 674–677.

Bajer, D., & Kaczmarek, H. (2010). Study of the influence OV UV radiation on biodegradable blends based on chitosan and starch. *Progress on Chemistry and Application of Chitin and its Derivative*, *15*, 17–24.

Baran, E. T., Mano, J. F., & Reis, R. L. (2004). Starch-chitosan hydrogels prepared by reductive alkylation cross-linking. *Journal of Material Science: Materials in Medicine*, *15*, 759–765.

Busilacchi, A., Gigante, A., Mattioli-Belmonte, M., & Muzzarelli, R. A. A. (2013). Chitosan stabilizes platelet growth factors and modulates stem cell differentiation toward tissue regeneration. *Carbohydrate Polymers*, *98*, 665–676.

Cael, J. J., Koenig, J. L., & Blackwell, J. (1973). Infrared and Raman spectroscopy of carbohydrates. Part III: Raman spectra of the polymorphic forms of amylose. *Carbohydrate Research*, *29*, 123–134.

Cael, J. J., Koenig, J. L., & Blackwell, J. (1975). Infrared and Raman spectroscopy of carbohydrates. Part VI: Normal coordinate analysis of V-amylose. *Biopolymers*, *14*, 1885–1903.

Calvo, P., Remunan-Lopez, C., Vila-Jato, J. L., & Alonso, M. J. (1997). Novel hydrophilic chitosan-polyethylene oxide nanoparticles as protein carriers. *Journal of Applied Polymer Science*, *63*, 125–132.

Chen, Y., Vellore Mohanraj, J., Fang, Wang., & Heather Benson, A. E. (2007). Designing chitosan–dextran sulfate nanoparticles using charge ratios. *AAPS PharmSciTech*, *8*, E1–E9.

Cho, Kwangjae, Wang, Xu, Nie, Shuming, Chen, Zhuo Georgia, & Shin, Dong M. (2008). Therapeutic nanoparticles for drug delivery in cancer. *Clinical Cancer Research*, *14*, 1310.

Choi, H., Chun, Y. S., Kim, S. W., Kim, M. S., & Park, J. W. (2006). Curcumin inhibits hypoxia-inducible factor-1 by degrading aryl hydrocarbon receptor nuclear translocator: A mechanism of tumor growth inhibition. *Molecular Pharmacology*, *70*, 1664–1671.

Das, Ratul Kumar, Kasoju, Naresh, & Bora, Utpal. (2010). Encapsulation of curcumin in alginate-chitosan-pluronic composite nanoparticles for delivery to cancer cells. *Nanomedicine: Nanotechnology, Biology and Medicine*, *6*, 153–160.

Dash, Suvakanta, Murthy, Padala Narasimha, Nath, Lilakantanath, & Chowdhury, Prasanta. (2010). Kinetic modeling on drug release from controlled drug delivery system. *Acta Poloniae Pharmaceutica Drug Research*, *67*, 217–223.

Debnath, S., Datta, D., Babu, M. N., Kumar, R. S., & Senthil, V. (2010). Studies on the preparation and evaluation of chitosan nanoparticles containing cytarbine. *International Journal of Pharmaceutical Sciences and Nanotechnology*, *3*, 957.

Francis, A. P., Dushendra Babu, G. J., Lavanya, M., Shenbaga Vidhya, K., & Devasena, T. (2011). Toxicity studies of aluminium oxide nanoparticles in cell lines. *International Journal of Nanotechnology and Applications*, *5*, 99–107.

Jhan, W. (1999). Chemical aspects of the use of gold clusters in structural biology. *Journal of Structural Biology*, *127*, 106–112.

Kumari, Kamalesh, & Rani, Usha. (2011). Controlled release of Metformin hydrochloride through cross linked blends of chitosan–starch. *Advances in Applied Science Research*, *2*, 48–54.

Lu, D. R., Xiao, C. M., & Xu, S. J. (2009). Starch-based completely biodegradable polymer materials. *Express Polymer Letters*, *3*, 366–375.

Muhammed Rafeeq, P. E., Junise, V., Saraswathi, R., Krishnan, P. N., & Dilip, C. (2010). Development and characterization of chitosan nanoparticles loaded with isoniazid for the treatment of Tuberculosis. *Research Journal of Pharmaceutical, Biological and Chemical Sciences*, *1*, 383–390.

Muzzarelli, R. A. A. (2009). Chitins and chitosans for the repair of wounded skin, nerve, cartilage and bone. *Carbohydrate Polymers*, *76*, 167–182.

Muzzarelli, R. A. A. (2010). Chitins and chitosans as immunoadjuvants and non-allergenic drug carriers. *Marine Drugs*, *8*, 292–312.

Muzzarelli, R. A. A., Tarsi, R., Filippini, O., Giovanetti, G., Biagini, G., & Varaldo, P. E. (1990). Antimicrobial properties of *N*-carboxybutyl chitosan. *Antimicrobial Agents and Chemotherapy*, *34*, 2019–2023.

Muzzarelli, R. A. A., Boudrant, J., Meyer, D., Manno, N., DeMarchis, M., & Paoletti, M. G. (2012). A tribute to Henri Braconnot, precursor of the carbohydrate polymers science, on the chitin bicentennial. *Carbohydrate Polymers*, *87*, 995–1012.

Naama, Jasim Hilo, Al-Temimi, Ali A., & Ahmed, A. Amiery Hussain. (2010). Study the anticancer activities of ethanoliccurcumin extract. *African Journal of Pure and Applied Chemistry*, *4*, 68–73.

Nagarwal, Ramesh Chand, Singh, ParasNath, Kant, Shri, Maiti, Pralay, & Pandit, Jayant Kumar. (2011). Chitosan nanoparticles of 5-fluorouracil for ophthalmic delivery: Characterization, in-vitro and in-vivo study. *Chemical and Pharmaceutical Bulletin*, *59*, 272–278.

Qi, L. F., Xu, Z. R., Jiang, X., Hu, C. H., & Zou, X. F. (2004). Preparation and antibacterial activity of chitosan nanoparticles. *Carbohydrate Research*, *339*, 2693–2700.

Qin, C. Q., Du, Y. M., Xiao, L., Li, Z., & Gao, X. H. (2002). Enzymatic preparation of water-soluble chitosan and their antitumor activity. *International Journal of Biological Macromolecules*, *31*, 111–117.

Rahman, Md Mofizur, Hasan, Sayeed, Alam, Md Ashiqul, Roy, Sumon, Jha, Mithilesh Kumar, Ahsam, Md Qamrul, & Rahman, Habibur Md. (2011). Formulation and evaluation of Ranolazine sustained release matrix tablets using Eudragit and HPMC. *International Journal of Pharmaceutical and Biomedical Research*, *2*, 7–12.

Roller, S., & Covill, N. (1999). The antifungal properties of chitosan in laboratory media and apple juice. *International Journal of Food Microbiology*, *47*, 67–77.

Shukla, P. K., Khanna, V. K., Ali, M. M., Khan, M. Y., & Srimal, R. C. (2008). Anti-ischemic effect of curcumin in rat brain. *Neurochemical Research*, *33*, 1036–1043.

Soundarajan, V., & Sreenivasan, S. (2012). Cytotoxicity of methanol extracts of Elaeisguineensis on MCF-7 and Vero cell lines. *Asian Pacific Journal of Tropical Medicine*, *2*, 826–829.

Stix, G. (2007). Spice healer. *Scientific American*, *296*, 66–69.

Strofer, M., Jelkmann, W., & Depping, R. (2011). Curcumin decreases survival of Hep3B liver and MCF-7 breast cancer cells: The role of HIF. *Strahlentherapie und Onkologie*, *187*, 393–400.

Thanou, M., Verhoef, J. C., & Junginger, H. E. (2001). Oral drug absorption enhancement by chitosan and its derivatives. *Advanced Drug Delivery Reviews*, *52*, 117–126.

Venkatraman, Shrinivas, Hedrick, James L., Ong, Zhan Yuin, & Yang, Chuan. (2011). The effects of polymeric nanostructures shape on drug delivery. *Advanced Drug Delivery Reviews*, *63*, 1228–1246.

Venugopal, Vazhiyil. (2011). *Marine polysaccharides: Food applications*. CRC Press.

Vidyanathan, R., Kalishwaralal, K., Gopalram, S., & Gurunathan, S. (2009). Nanosilver—The burgeoning therapeutic molecule and its green synthesis. *Biotechnology Advances*, *27*, 924–937.

Zhang, X. Q., Xua, X., Bertrand, N., Pridgenb, E., Swamia, A., & Farokhzad, O. C. (2012). Interactions of nanomaterials and biological systems: Implications to personalized nanomedicine. *Advanced Drug Delivery Reviews*, *64*, 1363–1384.

Zheng, L. Y., & Zhu, J. F. (2003). Study on antimicrobial activity of chitosan with molecular weights. *Carbohydrate Polymers*, *54*, 527–530.